Built-in reduction of statistical fluctuations of partitioning objects

E. DelRe,[1,2] B. Crosignani,[3] P. Di Porto,[2] and S. Di Sabatino[1]
[1]*Department of Electrical and Information Engineering, University of L'Aquila, I-67100 L'Aquila, Italy*
[2]*IPCF-CNR, University of Rome "La Sapienza," I-00185 Rome, Italy*
[3]*Department of Applied Physics, California Institute of Technology, Pasadena, California 91125, USA*
(Received 18 November 2010; revised manuscript received 21 June 2011; published 5 August 2011)

Our theoretical and numerical investigation of the movement of an object that partitions a microtubule filled with small particles indicates that vibrations warranted by thermal equilibrium are reached only after a time that increases exponentially with the number of particles involved. This points to a basic mechanical process capable of breaching, on accessible time scales, the ultimate ergodic constraints that force randomness on bound microscale and nanoscale systems.

DOI: 10.1103/PhysRevE.84.021112 PACS number(s): 05.70.Ln, 83.10.Rs

I. INTRODUCTION

Present-day instrumentation allows the control of matter from micrometer scales down to those of single molecules. Nanotechnology aspires to use this mastery to develop and harness qualitatively new functional systems composed of a small number of atoms. As scales get smaller, mechanical parts will jolt erratically even when they are bolted down, and thermal fluctuations become the dominant drive. These obey the ergodic hypothesis and are the result of averaging over all available phase space: as the system gets smaller, phase space contracts and averaging is less effective. The result is an unwanted increase in the relative amplitude of the fluctuations as the system becomes smaller [1]. Bound systems generally explore their phase-space rapidly, so that thermal fluctuations cannot be avoided and take over following a standard exponential law [2], unless extreme conditions such as dense packing and rapid cooling are implemented [3]. Nonergodic fluctuations can be observed in glass-like systems, where inhomogeneity and disorder preclude the possibility of exploring the whole phase space in observable times, a feature that can amount to a drastic alteration in statistical fluctuations [4]. The question lies open if nonergodicity and subthermal fluctuations can be found in a standard nano-sized mechanical system, providing a method to circumvent the basic stochastic feature associated to bound nanoscale objects.

Here we demonstrate how a wide class of bound microscopic mechanical systems can be made to manifest subergodic fluctuations even though they are normal, that is, they have no built-in disorder and associated glassy behavior. The paradigm system is an object that is topologically constrained to partition its small and agitated environment into two separate sections, as would occur for a Brownian particle sliding along and obstructing a tubule. The particle is bound to a specific position because of the continuous collisions of the opposing environments (microscopic embodiment of Boyle's law), but its fluctuations have novel and unexpected features that are in contrast with commonly held notions of bound fluctuating bodies. In fact, we find that thermal equilibrium is not reached with an exponential law typical of a single relaxation time constant [2]. Rather, equilibrium fluctuations are reached after a time that increases exponentially with the number of particles involved through a series of quasistationary plateaus that grow ever longer in time, amounting to a continuum of time scales. The result is that, on accessible time scales, the bound object fluctuates in space with subergodic quasistationary fluctuations.

II. PHASE-SPACE ANALYSIS

To demonstrate this subergodic behavior of partitioning particles, we consider the basic system illustrated in Fig. 1(a): an object (the large blue sphere) that slides along a microtubule and is in contact with N microscopic agitated particles (the red small spheres). The benchmark vibrations are the equilibrium fluctuations of the object position deduced by introducing the $(N+1)$-dimensional phase space, each point $x_1,x_2,\ldots,x_N,x$ of which corresponds to the positions of the N molecules and of the object (see Fig. 1(b)). The portion of phase-space volume $d\Gamma$ that corresponds to the object's position in a range dx depends on x through the constraint on the particle positions imposed by the object itself: $N/2$ particles in section A are confined in the region $(-L/2,x)$ and $N/2$ in section B in $(x,L/2)$. Accordingly, $d\Gamma = (L/2+x)^{N/2}(L/2-x)^{N/2}dx = (L/2)^N(1-4x^2/L^2)^{N/2}dx$, i.e., in the limit $N \gg 1$ and dropping the inessential constant $(L/2)^N$, $d\Gamma = \exp(-2Nx^2/L^2)dx$. The ergodic assumption requires the probability density $p(x)$ of the object being in the range dx to be proportional to the corresponding phase-space volume, that is $p(x) = (2N/\pi L^2)^{1/2}\exp(-2Nx^2/L^2)$, so that the normalized root-mean-square value of x is

$$\langle x^2\rangle_{\rm erg}^{1/2}/(L/2) = 1/\sqrt{N}. \tag{1}$$

Lower fluctuations can occur only if equilibrium is reached on inaccessibly long times. This is where the partitioning feature of the object intervenes: in so much that the internal degrees of freedom of the body do not intervene, particles in section A are never directly in contact with particles in section B, and their mutual interaction is forced to occur through collisions with the single rigid vibrating object. Even though the most probable energy exchange mechanism involves successive alternate collisions with an A and a B particle on the object, for complete ergodicity to occur, the passage of energy from one section to the other must also involve extremely less probable events, such as those in which a finite number of particles from one section collide

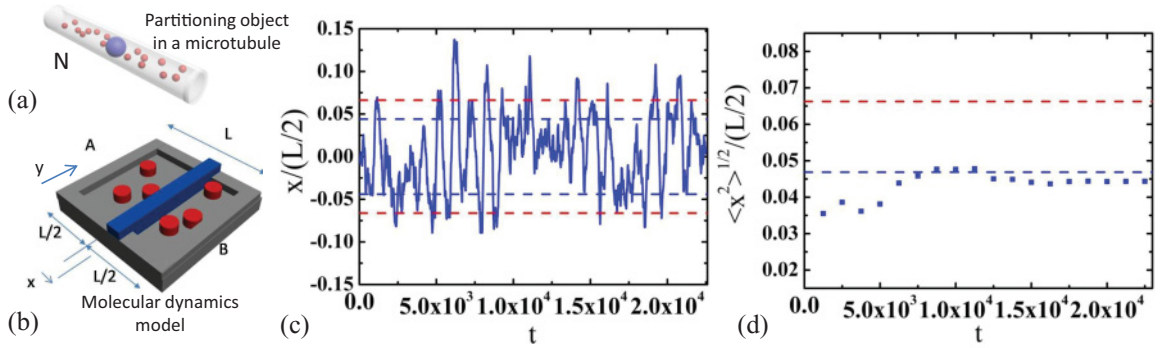

FIG. 1. (Color online) Partitioning object in a microtubule and reduced vibrations. (a) General layout of an object (large blue sphere) sliding along a microtubule filled with smaller particles (red spheres). (b) Molecular dynamics scheme. (c) Example of the object trajectory $x(t)/(L/2)$ (full blue curve) for $N = 200$, $m = 1$, and $M = 20$. Superimposed are the values of $x/(L/2) = \pm 1/\sqrt{N}$ (top and bottom red dashed lines) and $x/(L/2) = \pm 1/\sqrt{2N}$ (blue dashed lines), corrected for the effect of the finite covolume [15]. (d) Fluctuations are evaluated through the corresponding value of $\langle x^2\rangle^{1/2}/(L/2) = \{(1/t)\int_0^t [x(t')/(L/2)]^2 dt'\}^{1/2}$ (root-mean square of the object position), which saturates to the value 0.045 (blue squares) considerably lower than the ergodic expectation $1/\sqrt{N} \simeq 0.071$ (0.066 taking into account the finite covolume [15], red dashed line). The approach to this first quasiequilibrium indicates a $t_p \simeq 2 \times 10^4$. For $N < 200$, see Fig. 3(b) and its discussion.

with the object while no particle from the other side hits it. More precisely, the time to reach ergodicity can be estimated as that required for a relative energy fluctuation, from one section to the other, of the order of $1/\sqrt{N/2}$, to occur [5]. This requires a $\sqrt{N/2}$-particle event, i.e., a sequence of $\sqrt{N/2}$ collisions occurring on the object from only one of the two sections, and hence a time $2^{\sqrt{N/2}} t_p$, where t_p is the characteristic thermalization-time for each separate section (the microscopic time scale associated to normal gas/liquid systems). Hence, on experimentally available times, the object will fluctuate on the basis of a partial set of dynamical events in which the improbable collisions are absent (weak ergodicity breaking) [6,7]. For a small enough partitioning object [7], the ergodic equilibrium is simply a theoretical limit that will be practically violated. To grasp how this leads to subergodic fluctuations [i.e., below the limit of Eq. (1)], consider the situation in which all the less probable asymmetric collisional events are neglected. This means neglecting large pressure fluctuations and corresponds to the quasiequilibrium regime conjectured in adiabatic piston models, for which the pressure in the two sections is assumed equal [8–13]. In turn, equal pressures imply that the maximum energy of the single particles in A and B is correlated to the position x of the object, because its value is now proportional to $(L/2 + x)$ in A and to $(L/2 - x)$ in B. In other words, the correlation between the maximum energy of the single particles and the object position implies maximum values of their momentum p_x and p_y proportional to $(L/2 + x)^{1/2}$ for the particles in A, and $(L/2 - x)^{1/2}$ for the particles in B. This modifies the phase space available to each particle from $(L/2 + x)$ to $(L/2 + x)^{(1+1/2+1/2)} = (L/2 + x)^2$ (particles in A), and $(L/2 - x)^2$ (particles in B). The resulting motion suffers a partially ergodic dynamic associated with the volume $d\Gamma = (L/2 + x)^N (L/2 - x)^N dx = (L/2)^{2N}(1 - 4x^2/L^2)^N dx$. Thus, in the limit $N \gg 1$ and dropping inessential factors, $d\Gamma = \exp(-4Nx^2/L^2)dx$. The probability density is now $p(x) = (4N/\pi L^2)^{1/2} \exp(-4Nx^2/L^2)$, and the fluctuations are reduced by a factor $1/\sqrt{2}$, which leads to the subergodic result

$$\langle x^2\rangle^{1/2}/(L/2) = 1/\sqrt{2N}. \tag{2}$$

III. MOLECULAR DYNAMICS

To detect these reduced fluctuations we carry out molecular dynamics (MD) simulations on the flat system illustrated in Fig. 1(b). The partitioning object is therefore a rigid segment of mass M (the blue wall) and side L that slides along one axis (the x axis) of a square of side L (the microtubule). The opposing agitated molecular environment is composed of a gas of diluted N rigid disks of mass m (the red disks) contained in the microtubule and separated into two closed compartments, A and B, each containing $N/2$ disks, by the sliding particle [14].

A typical trajectory of the object is shown in Fig. 1(c) (full blue curve). Analyzing the stochastic process, we find (see Fig. 1(d)) the remarkable result that the system undergoes a quasi-stationary initial dynamic phase that settles to a value for the fluctuations in position $\langle x^2\rangle^{1/2}/(L/2) \simeq 0.045$. This result is consistent with the subergodic behavior described in Eq. (2), smaller by a factor $1/\sqrt{2}$ than the ergodic value $\simeq 0.071$ predicted by Eq. (1).

The equal pressure condition leading to Eq. (2) is tested in Fig. 2, where we compare the values of the total energy in section A, $E_A(t)$, and that in section B, $E_B(t)$, normalized to the total energy in the system $E_A + E_B = E_0$, with the object position $x(t)$ (blue squares) for the case of the dynamics reported in Fig. 1. Comparing the averaged values of $\langle E_A(t)\rangle$, $\langle E_B(t)\rangle$ and $\langle x(t)\rangle$ along the trajectory indicates a direct average proportionality between the volume of each section [i.e., for A, $L(x + L/2)$, and for B, $L(-x + L/2)$] and the energy there contained. This corresponds to a movement of the object in conditions in which the pressures in the two sections are loosely equal and constant, and is a signature of

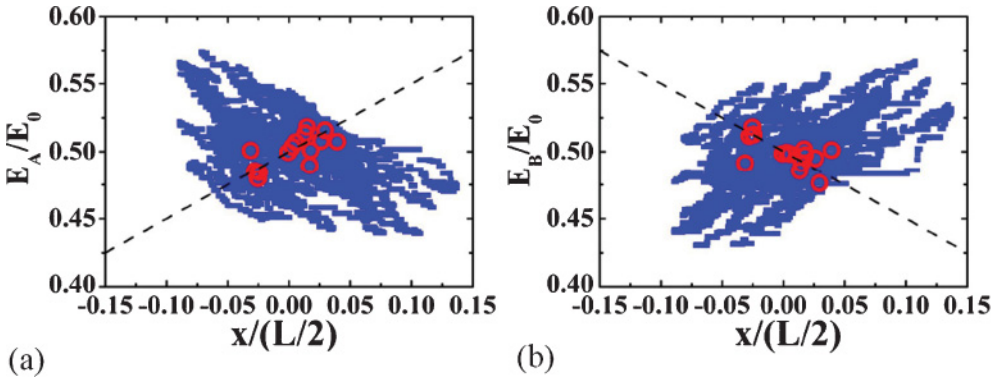

FIG. 2. (Color online) Phase-space analysis of $x(t)$ and detection of occupation-time anomalies. (a) Plot of $E_A(t)/E_0$ [$E_A(t)$ is the total energy in section A] versus $x(t)/(L/2)$ (blue squares), that shows that for average values (taken over intervals of $\Delta t = 1250$, red circles) an approximate and loose validity of an "equation of state" holds, i.e., $E_A/E_0 = (1/2)[x/(L/2)] + 1/2$ (black dashed line). (b) The same analysis for $E_B(t)/E_0$ [where correspondingly $E_B(t)$ is the total energy of section B].

the occupation-time anomaly at the basis of the breaking of ergodicity.

For limited values of N the breakdown of ergodicity can be directly observed (by suitably expanding the duration of the MD simulation), while this is practically impossible for larger values of N. For the still tractable case of $N = 200$, using an event-driven MD (see for example [16]), we are able to span the entire phase space, thus achieving the final ergodic result predicted by Eq. (1), by increasing the time window by more than 6 orders of magnitude with respect to the observed first asymptotic-like subergodic behavior of Fig. 1(d). The results are reported in Fig. 3(a) and have remarkable features. Even though the system is composed of extremely simple rigid and diluted particles, it reproduces in its fluctuations (and, through

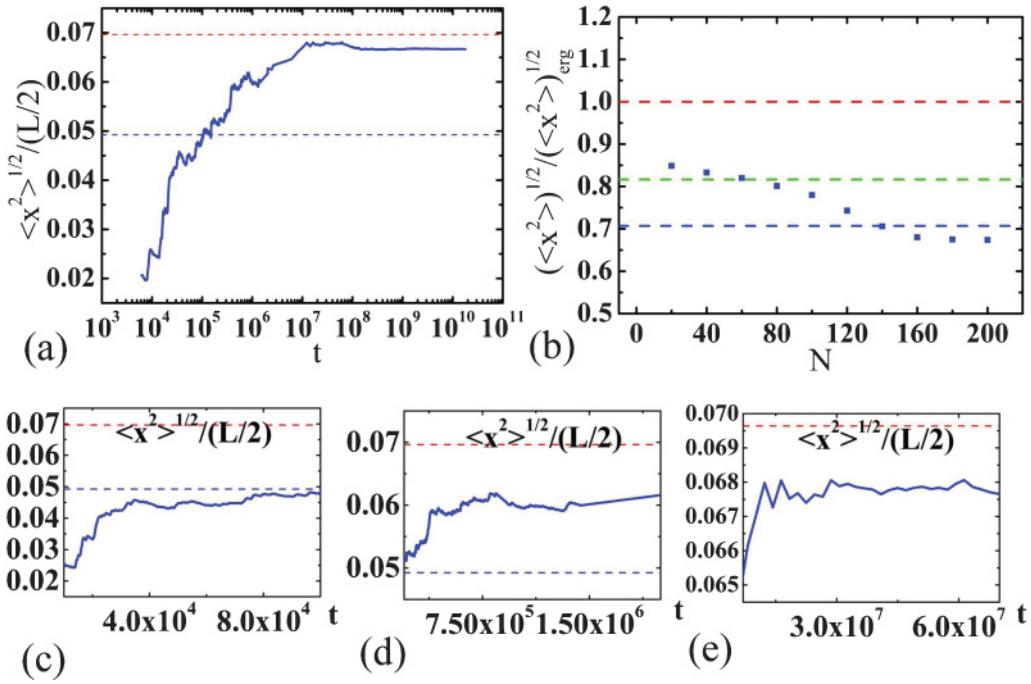

FIG. 3. (Color online) Complexity: a self-similar and ever slower approach to equilibrium. (a) The blue line represents the evolution of $\langle x^2\rangle^{1/2}/(L/2)$ for a sample in the conditions of the run of Fig. 1 ($N = 200$, the mass of the object $M = 20$). The short time region ($t \sim t_p$) below the lower blue dashed line [the $n = 2$ prediction of Eq. (3)] is where the condition of practical equilibrium is reached and violates the $1/\sqrt{N}$ law. In this regime only the probable molecule-molecule interaction events in the separate sections/partitions are active, and weak ergodicity breaking occurs. The second long time ($t > t_p$) region above the lower blue dashed line is so long that even the increasingly improbable events involving energy/information transfer through the object partake in the dynamics, leading to the restoration of ergodicity (top red dashed line). (b) Comparison of MD results (blue squares) to the ergodic prediction of Eq. (1) (top red dashed line) and the nonergodic prediction for different values of N, middle green dashed line for $n = 1$ and lower blue dashed line for $n = 2$ [see Eq. (3) and discussion thereafter], for the quasiequilibrium condition, first plateau in the evolution of (a). (c,d) Fluctuations follow a power-law, as highlighted by the self-similarity observed at different time scales in the linear time plots of (c), (d), and (e).

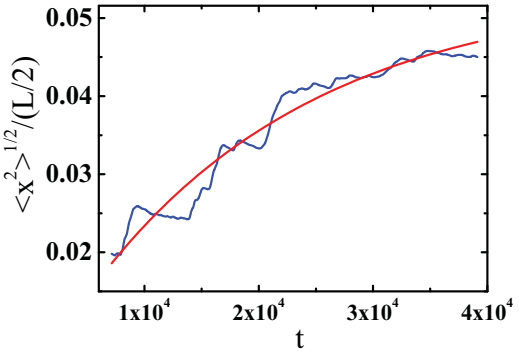

FIG. 4. (Color online) Short time region of trajectory reported in Fig. 3(a) fitted with an exponential law of the type $\langle x^2\rangle^{1/2}/(L/2) \propto 1 - \exp(-t/t_p)$, with $t_p \simeq 19.5 \times 10^3$.

the fluctuation-dissipation theorem, in its relaxation processes [17]) *the basic signatures of complexity* [6]. For short times ($t \sim t_p$), fluctuations are compatible with an exponential-like law as reported in Fig. 4. For long time scales ($t \gg t_p$), the nonlinear behavior in the logarithmic plot indicates a *power-law* behavior, with **no** characteristic time scale. This is evidenced by the self-similarity of time evolution (see Figs. 3(c)–3(e)).

IV. DISCUSSION

The dimensionality of the system determines the amplitude of the reduction in the spontaneous fluctuations: each successive quadratic energy term that thermalizes in each section separately becomes correlated to x and adds in the phase space $d\Gamma$ a factor $(L/2 + x)^{1/2}$ for each particle in A, and $(L/2 - x)^{1/2}$ for each particle in B. This change of $d\Gamma$ generalizes Eq. (2) into

$$\langle x^2\rangle^{1/2}/(L/2) = 1/\sqrt{(2+n)N/2}, \tag{3}$$

where n is the number of quadratic energy terms: more degrees of freedom will induce a stronger fluctuation reduction.

To investigate the size dependence of the subergodic regime and to validate the result of Eq. (3), we analyze $\langle x^2\rangle^{1/2}/(L/2)$ as a function of N. As shown in Fig. 3(b), first plateau results (weak ergodicity breaking) are in good agreement with the prediction of Eq. (2) for $N = 200$ while, for decreasing N, $\langle x^2\rangle^{1/2}/(L/2)$ tends to the value given by Eq. (3) for $n = 1$. This is caused by the reduced number of particle-particle collisions which in turn implies that the thermalization process occurs predominantly through particle-object collisions, which affect only momentum exchange along x, so that y-velocity thermalization is ineffective over reasonable times. Congruently, this implies a progressive change of n from $n = 2$ to $n = 1$ in Eq. (3) as N decreases.

The reduction in spontaneous fluctuations can have far-reaching practical implications in many areas of microscience, providing insight into the workings of microengines embedded in a noisy environment, and into the ultrasensitive sensors. For example, it could favor the preservation of quantum coherence in living cells [18]. To get an estimate of the effect, consider microtubules in the cellular cytoskeleton, i.e., polymeric tubes composed of the tubulin protein of varying length and a 15 nm internal diameter, normally associated to biased Brownian motion occurring on their external surface [19]. Consider a single microtubule with $L = 50$ nm, hosting (on the inside) a partitioning colloidal sphere (the object) of 15 nm diameter and $N = 200$ colloidal particles of 1 nm diameter, of mass $m = 0.5 \times 10^{-24}$ Kg, at $T = 300$ K. When the mass of the partitioning object is $M = 20m$, subergodic fluctuations (first plateau in Fig. 1(d)) are reached in a time $t_p \simeq 1\,\mu$s, remain fixed to the basic correction of Eq. (2) (the actual value will depend on the value of n of the system) on the scale of 10 μs, and grow at an ever slower rate, to reach the ergodic fluctuations on a scale of 1 s (Fig. 3(a)). We note that the presence of the fluidic medium hosting the particles may play a significant role, in which case a more detailed model of the system must be invoked. It should, however, be noted that from a conceptual perspective, our results indicate the unexpected emergence of complex behavior for rigid-particle systems even in the highly diluted regime and without dispersion in their radius, suggesting a basic role in complex phenomena for partitioning topologies. In evaluating the relevance of our results, we must underline that the reduction in vibrations turns out to be a robust property in that it is only dependent on the presence of partitioning objects. For example, for $N_A \neq N_B$ fluctuations around the equilibrium position [at a distance $LN_A/(N_A + N_B)$ from the fixed wall of section A] turn out to be $\langle x^2\rangle^{1/2}_{\rm erg}/(L/2) = 2/(N\sqrt{1/N_A + 1/N_B})$ and $\langle x^2\rangle^{1/2}/(L/2) = (2)^{-1/2}\langle x^2\rangle^{1/2}_{\rm erg}/(L/2)$, where $N = N_A + N_B$, that respectively generalize Eqs. (1) and (2). Analogously, when an external force contributes to bind the object to the equilibrium position. In fact, introducing the external potential $V(x) = (1/2)kx^2$, Eqs. (1) and (2) generalize into $\langle x^2\rangle^{1/2}_{\rm erg}/(L/2) = \{2k_BT/[2k_BTN + k(L/2)^2]\}^{1/2}$ and again $\langle x^2\rangle^{1/2}/(L/2) = (2)^{-1/2}\langle x^2\rangle^{1/2}_{\rm erg}/(L/2)$. In general, our findings can be extended to a network of interconnected microtubules with numerous partitioning objects, so that even the condition that the microtubules are closed at the end can have a negligible influence.

Fruit of topology, the weak-ergodicity breaking is expected also in different systems, such as nanomagnets riddled by Johnson noise, where they could significantly increase storage capacity. In the microtubule, information can be stored in the position of the object (using $N_A \neq N_B$). At each specific equilibrium position $X = LN_A/(N_A + N_B)$ (measured from the top of the tubule in section A), the $\langle x^2\rangle^{1/2}$ in the ergodic case is expressed as function of X and the number of distinguishable states (i.e, separated by a distance $\langle x^2\rangle^{1/2}$) is $n^{\rm erg}_{\rm bits} \simeq \int_0^L dX\sqrt{N/[X(L-X)]} = \pi\sqrt{N}$. In the subergodic case, this number is increased to $n_{\rm bits} = \sqrt{2}n^{\rm erg}_{\rm bits}$.

V. CONCLUSIONS

In conclusion, we have demonstrated that a microscopic object partitioning a microtubule evolves toward equilibrium with no characteristic time scale, following a sequence of quasiequilibrium states that globally lasts for an interval of time that grows exponentially with $\sqrt{N/2}$. The result is that the bound object fluctuates in a notably subergodic manner on accessible intervals of time.

ACKNOWLEDGMENTS

Authors are grateful for useful discussion with Claudio Conti. Research was carried out through funding from the Italian Ministry of Research (MIUR) through the Futuro in Ricerca FIRB-grant PHOCOS - RBFR08E7VA. Partial funding was received through the SMARTCONFOCAL project of the Regione Lazio (FILAS grant).

[1] K. Pathria, *Statistical Mechanics* (Butterworth, Oxford, 1996).

[2] S. Chandrasekhar, Rev. Mod. Phys. **15**, 1 (1943).

[3] P. N. Pusey, E. Zaccarelli, C. Valeriani, E. Sanz, W. C. Poon, and M. E. Cates, Philos. Trans. R. Soc. London A **367**, 4993 (2009).

[4] L. Leuzzi and T. M. Nieuwenhuizen, *Thermodynamics of the Glassy State* (Taylor and Francis, New York, 2008).

[5] This allows enough events to build up a significant probability distribution.

[6] J. P. Bouchaud, J. Phys. I France **2**, 1705 (1992).

[7] It can be readily demonstrated in general that this hierarchy of improbable events disappears as the size of the system increases, so that thermal equilibrium of Eq. (1) is reached with an ordinary exponential law. This can be attributed to the role played by the internal degrees of freedom of the body in mediating energy transfer from A to B.

[8] H. B. Callen, *Thermodynamics* (Wiley, New York, 1960).

[9] R. P. Feynman, R. Leighton, and M. Sands, *The Feynman Lectures on Physics I*, Chap. 39. (Addison-Wesley, Reading, MA, 1963).

[10] B. Crosignani, P. Di Porto, and M. Segev, Am. J. Phys. **64**, 610 (1996).

[11] E. H. Lieb, Physica A **263**, 491 (1999).

[12] For a full list of references on the adiabatic piston, see P. Castiglione, M. Falcioni, A. Lesne, and A. Vulpiani, *Chaos and Coarse Graining in Statistical Mechanics* (Cambridge University Press, Cambridge, 2008).

[13] Pressure fluctuations participate in the dynamics since they hold the particle bound to $x = 0$: the point is that on short time scales, the average condition $p_A = p_B$ holds (without in this manner implying that the energies in the two sections are equal), a condition that is washed out on the very long time scales that ultimately lead to the ergodic equilibrium of Eq. (1) shown in Fig. 2, where now the condition of equal temperatures in the two sections sets in. This condition is stronger than the equal pressure condition, which it evidently includes.

[14] In the MD, at $t = 0$ the N particles are attributed a random initial velocity from a Maxwell distribution compatible with an equal total energy in the sections, $E_A(t = 0) = E_B(t = 0) = E_0/2$. The object starts from the central position (dividing the square in two) $x(t = 0) = 0$ with initial zero velocity. Simulations are carried out for a 50×50 spatial lattice, with each microscopic molecule of unit diameter $\sigma = 1$, initial Maxwell distribution with $(\langle v_x^2 \rangle)^{1/2} = (\langle v_y^2 \rangle)^{1/2} = 25$ per unit time. The value of L, m, and E_0 determines the unit of time through the relationship $(1/2)m\langle v_x^2 \rangle = (E_0/2)/N$.

[15] Considering the relative covolume $\epsilon = (N\pi\sigma^2/8)/(L^2/2)$, the finite size of the disks entails that the spatial component of the phase space volume for a single disk reads $L(L/2 + x) - L(L/2)\epsilon$ (for section A), and $L(L/2 - x) - L(L/2)\epsilon$ (for section B). All equations, and hence Eq. (2), are approximately modified by substituting L with $L(1 - \epsilon)$ in the actual predictions. For example, for the observations in Fig. 1, $\epsilon \simeq 0.06$. Note that a more sophisticated approach (not explicitly addressed here) based on the analysis proposed in J. A. Barker and D. Henderson, Rev. Mod. Phys. **48**, 587 (1976), indicates that L should be modified to $L(1 - 2\epsilon)$, which results in an even better agreement with data.

[16] D. C. Rapaport, J. Comput. Phys. **34**, 184 (1980).

[17] H. B. Callen and T. A. Welton, Phys. Rev. **83**, 34 (1951).

[18] S. Hameroff and R. Penrose, Math. Comput. in Simul. **40**, 453 (1996).

[19] R. Lipowsky, S. Klumpp, and T. M. Nieuwenhuizen, Phys. Rev. Lett. **87**, 108101 (2001).